Research Article *Open Access*

Journal of Modern Classical Physics & Quantum Neuroscience

ISSN: 3068-4196

DOI: *doi.org/10.63721/26JPQN0157*

Communication: Phase Diagram, Microstructure and Atomistic 2nd Law of Thermodynamics

Kuo-Chung Liu

Independent Researcher (Retired), Taiwan

Citation: *Kuo-Chung Liu (2026) Communication: Phase Diagram, microstructure and Atomistic 2nd Law of Thermodynamics. J. of Mod Phy & Quant Neuroscience 2(2), 1-12. WMJ/JPQN-157*

Abstract

The Atomistic 2nd Law of Thermodynamics and its necessary and sufficient condition can be used to explain the phase diagrams of one or two components. In these explanations, the molar total chemical potentials of atomistic features play important roles, while the common tangent and lever rule are useful. In explaining the microstructural evolution at a composition of a binary phase diagram, the driving force, mobility of atomistic features and lever rule etc. are applied. Recently the use of machines or AI in the optimization of material properties is highly valued. More effective results could be obtained if the user of these tools have better understanding of the Atomistic 2nd Law of Thermodynamics and kinetics. The discussed topics are: T-T-T curve, T-T-T curve of 1080 steel, T-T-T of other materials, contains low-melting impurities.

***Corresponding author**: Kuo-Chung Liu, Independent Researcher (Retired), Taiwan.

Submitted: 17.03.2026 **Accepted**: 23.03.2026 **Published**: 31.03.2026

Keyword: Phase Diagram, Atomistic Thermodynamics, Chemical Potential, Microstructure, Property, Ai, T-T-T Curve, Driving Force, Mobility, Slags

Introduction

The rule of the Atomistic 2nd Law of Thermodynamics is: without other driving forces (e.g. mechanical stirring, external ΔP in reverse osmosis or blood pressure), the molar total potential of atomistic features of a system is the lowest at spontaneous equilibrium. The necessary and sufficient condition of this rule is: the molar total potential is equal everywhere in the system. When the potentials other than chemical potential, e.g. gravitational potential, electrical potential, magnetic potential, can all be neglected, the term of "molar total potential" becomes "molar total chemical potential".

Phase diagrams are to display the equilibrium phase(s) in a system under various conditions such as temperature, pressure and composition. Equilibrium can be achieved via two ways. One way is: the molar total chemical potential of atomic species is at minimum or the Atomistic 2nd Law of Thermodynamics itself; the second

way is: all equilibrium phases have the same molar total chemical potential, i.e. the necessary and sufficient condition of the Atomistic 2nd Law of Thermodynamics. One-component phase diagrams comply with both.

A typical binary phase diagram includes the following:

- Single phase zones: at various temperature, the molar total chemical potential of the system is lowered due to the dissolution of one component into the other (the molar total chemical potential is the lowest when the dissolution is saturated);
- Co-existing zones of two phases: at the co-existing composition and temperature, the molar total chemical potential is the lowest in the system;
- Eutectic (or Eutectoid) point: at this composition and temperature, the molar total chemical potential is the lowest in the system;
- Boundaries of single phases: at the composition and temperature indicated, the molar total chemical potential is the lowest in the system. Hence, binary phase diagrams also have close relation with the Atomistic 2nd Law of Thermodynamics.

Some documents showed binary phase diagrams together with the evolution of microstructures at certain composition. Although these figures are helpful to understand the relation between microstructures and phase diagrams, an in-depth explanation is not offered. The author believes, phase diagrams and their near equilibrium microstructures can be well explained via the Atomistic 2nd Law of Thermodynamics and its necessary and sufficient condition as well as kinetics. The following are some studies related to these topics.

Phase diagrams and the Atomistic 2nd Law of Thermodynamics

The analyses in this section are mostly for binary phase diagrams, while for one-component or three-component the descriptions on phase diagrams are only brief.

One Component

For the phase diagrams of one-component, normally the X-axis is temperature, whereas the Y-axis is pressure. Fig.1 is the phase diagram for water [3]:

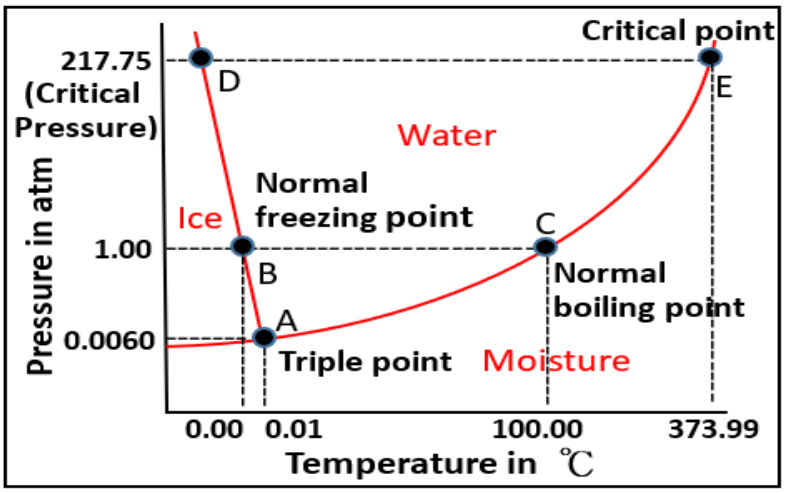

Figure1: Phase diagram for water.

In Figure.1, the equilibrium single phase areas for ice, water and moisture show the molar chemical potential for water molecules is the lowest in the system at various temperatures and pressures. Fig.1 also shows there are two red curves separating ice, water and moisture. The phases on the two sides of red curves are at equilibrium at the temperatures and pressures indicated by the red boundaries, because both phases have the same molar chemical potential.

For example, ice and water are at equilibrium at 1atm and 0°C (point B), and water and moisture are at equilibrium at 1atm and 100°C (point C); while all 3 phases are at equilibrium at 0.0060atm and 0.01°C (triple point A). Fig.1 also shows: when the pressure is less than 1atm (e.g. at mountains), water will boil at a temperature less than 100°C.

Another example is in the phase diagram of carbon, it is known that at room temperature and pressure the stable phase is graphite, and diamond is metastable (like glass). Diamond is unable transforming to graphite and can be kept forever at room temperature and pressure due to kinetic constrains. According to the phase diagram of carbon [4], at very high pressure diamond is at equilibrium with diamond plus metastable graphite.

Two-component A and B[3]

When B dissolves in A as α phase, according to the Atomistic 2nd Law of Thermodynamics, the molar total chemical potential of α phase at composition X (denoted as $\mu_\alpha(X)$) will decrease with increased X_α. When $X>X_\alpha$, $\mu_\alpha(X)$ will increase again. As a result, $\mu_\alpha(X)$ is a concave upward curve with composition X. Similarly, the $\mu_L(X)$ of liquid phase and the $\mu_\beta(X)$ of β phase are also concave upward curves with composition X, as shown in Figure 2.

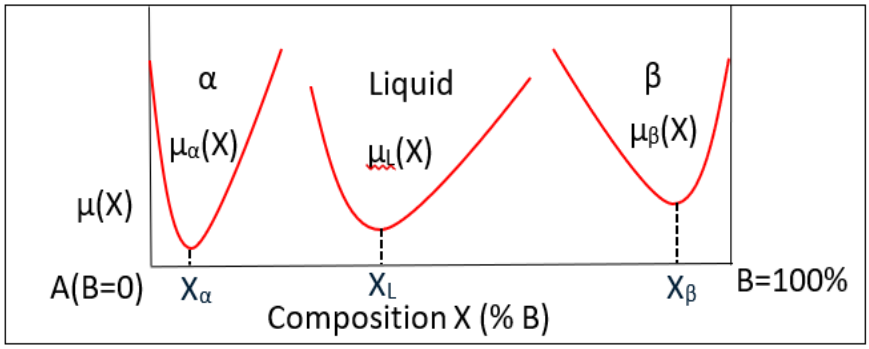

Figure 2: The μ(X) of α, β and L phases are all concave upward curves.

In a typical binary phase diagram, normally X-axis is composition, Y-axis is temperature, while pressure is kept at 1atm. Fig.3 [5] is a binary phase diagram with components A and B which has several single-phase zones (i.e. liquid L, α phase, β phase), an Eutectic composition, an Eutectic temperature, several co-existing zones as well as some boundaries.

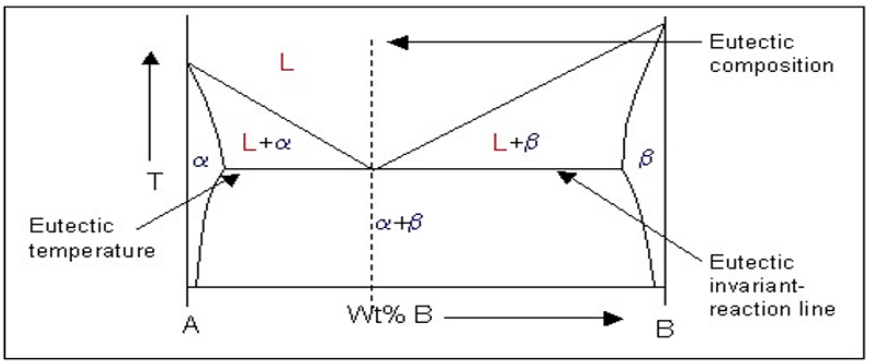

Figure 3: A typical binary phase diagram with components A and B.

At Eutectic Temperature

Based on the Atomistic 2nd Law of Thermodynamics, at this temperature the molar total chemical potential of composition X between A and B (denoted by μ(X)) is the lowest. Hence, according to Fig.3, μ(X) comes from α, Liquid+α, Liquid+β and β when X increases. This is shown as the red curve of Fig.4 (E denotes Eutectic

point, XLE denotes Eutectic composition):

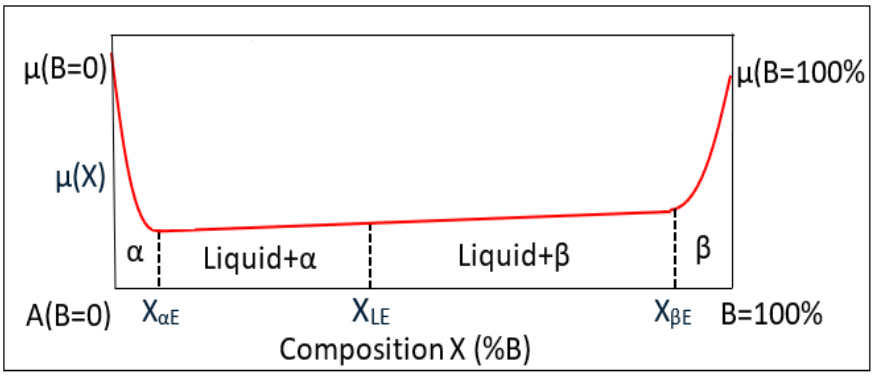

Figure 4: The red curve is the lowest μ(X) between A and B at Eutectic temperature.

I.e. μ(X) is as follows:

When $0 \leqq X \leqq X_{\alpha E}$, $\mu(X)=\mu_{\alpha}(X)$,

When $X_{\alpha E} \leqq X \leqq X_{\beta E}$, $\mu(X)=\mu_{\alpha}(X_{\alpha E})+\{[\mu_{\beta}(X_{\beta E})-\mu_{\alpha}(X_{\alpha E})] \div (X_{\beta E}-X_{\alpha E})\} \cdot (X-X_{\alpha E})$,

When $X_{\beta E} \leqq X \leqq 100\%$, $\mu(X)=\mu_{\beta}(X)$ (Eq.1)

The characteristics of (Eq.1) include:

- $[\mu_{\beta}(X_{\beta E})-\mu_{\alpha}(X_{\alpha E})] \div (X_{\beta E}-X_{\alpha E})$ is the slope of the common tangent in Liquid+α zone as well as in Liquid+β zone. In this equation $\mu_{\beta}(X_{\beta E})$, $\mu\alpha(X_{\alpha E})$, $X_{\beta E}$, and $X_{\alpha E}$ are all constants.
- Lever rule can be applied to the co-existing zones: for example when $X_{\alpha E} \leqq X \leqq XLE$, the ratio of Liquid phase is (X-XαE)÷(XLE-XαE). Similarly when $X_{LE} \leqq X \leqq X_{\beta E}$, the ratio of β phase is $(X-X_{LE}) \div (X_{\beta E}-X_{LE})$.

At temperatures slightly higher than Eutectic temperature

At this temperature, liquid is in a single-phase zone. Similar to at Eutectic temperature, Fig.3 shows the lowest μ(X) between A and B comes from α1 phase, Liquid+α1 zone, Liquid phase, Liquid+β1 zone and β1 phase when X increases, as shown in the red curve of Fig.5:

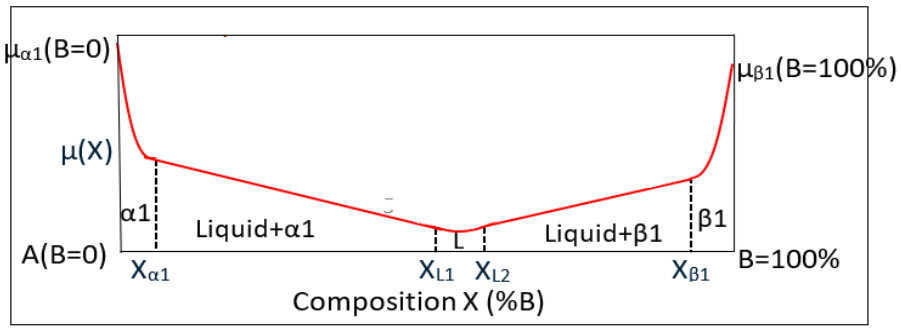

Figure 5: The red curve is the lowest μ(X) between A and B in this case.

I.e. μ(X) is as follows:

When $0 \leqq X \leqq X_{\alpha 1}$, $\mu(X)=\mu_{\alpha 1}(X)$,

When $X_{\alpha 1} \leqq X \leqq X_{L1}$, $\mu(X)=\mu_{\alpha 1}(X_{\alpha 1})+\{[\mu_{L}(X_{L1})-\mu_{\alpha 1}(X_{\alpha 1})] \div (X_{L1}-X_{\alpha 1})\} \cdot (X-X_{\alpha 1})$,

When $X_{L1} \leqq X \leqq X_{L2}$, $\mu(X)=\mu_{L}(X)$,

When $X_{L2} \leqq X \leqq X_{\beta 1}$, $\mu(X)=\mu_{L}(X_{L2})+\{[\mu_{\beta 1}(X_{\beta 1})-\mu_{L}(X_{L2})] \div (X_{\beta 1}-X_{L2})\} \cdot (X-X_{L2})$,

When $X_{\beta 1} \leqq X \leqq 100\%$, $\mu(X)=\mu_{\beta 1}(X)$ (Eq.2)

The characteristics of (Eq.2) include:

- $[\mu_L(X_{L1})-\mu_{\alpha 1}(X_{\alpha 1})]\div(X_{L1}-X_{\alpha 1})$ is the slope of the common tangent in Liquid+α1 zone; while $[\mu_{\beta 1}(X_{\beta 1})-\mu_L(X_{L2})]\div(X_{\beta 1}-X_{L2})$ is the slope of the common tangent in Liquid+β1 zone.
- Lever rule can be applied: when $X_{\alpha 1} \leqq X \leqq X_{L1}$, the ratio of Liquid phase is $(X-X_{\alpha 1})\div(X_{L1}-X_{\alpha 1})$. Similarly, when $X_{L1} \leqq X \leqq X_{\beta 1}$, the ratio of β1 phase is $(X-X_{L1})\div(X_{\beta 1}-X_{L1})$.
- In Fig.3, since the boundaries of Liquid+α1 zone and Liquid+β1 zone are not vertical, $X_{\alpha 1} \neq X_{\alpha E}$, $X_{\beta 1} \neq X_{\beta E}$, phase α1≠phase α, phase β1≠phase β.

At temperatures slightly lower than Eutectic temperature

In this case Fig.3 shows the equilibrium phases are only α2 phase, α2+β2 zone and β2 phase. Similarly, between A and B the lowest μ(X) comes from α2 phase, α2+β2 zone and β2 phase when X increases, as shown in Fig.6:

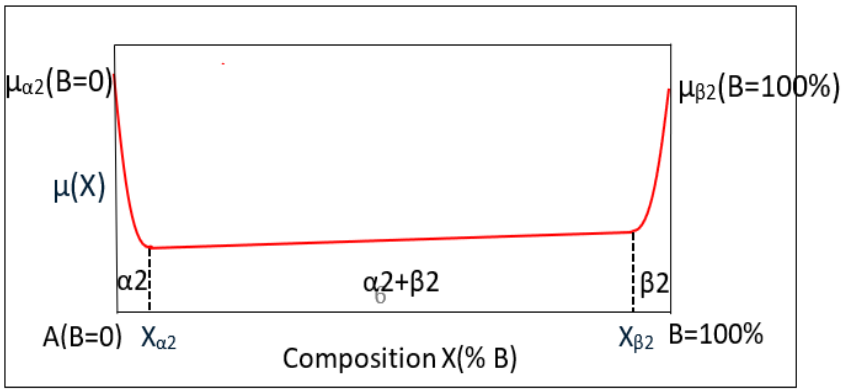

Figure 6: The red curve is the lowest μ(X) between A and B in this case.

I.e. μ(X) is as follows:

When $0 \leqq X \leqq X_{\alpha 2}$, $\mu(X)=\mu_{\alpha 2}(X)$

When $X_{\alpha 2} \leqq X \leqq X_{\beta 2}$, $\mu(X)=\mu_{\alpha 2}(X_{\alpha 2})+\{[\mu_{\beta 2}(X_{\beta 2})-\mu_{\alpha 2}(X_{\alpha 2})]\div(X_{\beta 2}-X_{\alpha 2})\}\cdot(X-X_{\alpha 2})$

When $X_{\beta 2} \leqq X \leqq 100\%$, $\mu(X)=\mu_{\beta 2}(X)$ (Eq.3)

The characteristics of (Eq.3) include:

(a) $[\mu_{\beta 2}(X_{\beta 2})-\mu_{\alpha 2}(X_{\alpha 2})]\div(X_{\beta 2}-X_{\alpha 2})$ is the slope of the common tangent in α2+β2 zone.

(b) Lever rule can be applied to α2+β2 zone: when $X_{\alpha 2} \leqq X \leqq X_{\beta 2}$, the ratio of phase β2 is $(X-X_{\alpha 2})\div(X_{\beta 2}-X_{\alpha 2})$.

(c) In Fig.3, since the boundaries of α2+β2 zone are not vertical, $X_{\alpha 2} \neq X_{\alpha E}$, $X_{\beta 2} \neq X_{\beta E}$, and phase α2≠phase α1, phase β2≠phase β1.

Three-Component

When there are three components in a system, the phase diagrams become quite complicated although the basic rules are the same. In this condition, normally temperature and pressure are fixed, and each side of a triangle is used for the compositions of each component. Reference [6] has detailed explanations for ternary phase diagrams.

In Co-Ti-Ta system, Wang et al [7] displayed three binary phase diagrams to show the relations among these three components. Electron probe micro-analyzer and X-ray diffraction were used as tools for their experimental verification.

Microstructure and Phase Diagram

Evolution of Microstructure in Pb-Sn alloy

When the microstructural evolution at one composition is shown together with a binary phase diagram, it's convenient to study the relation between them. Fig.7 is an example showing the phase diagram of Pb-Sn alloy and the microstructural evolution at composition C_4 [8].

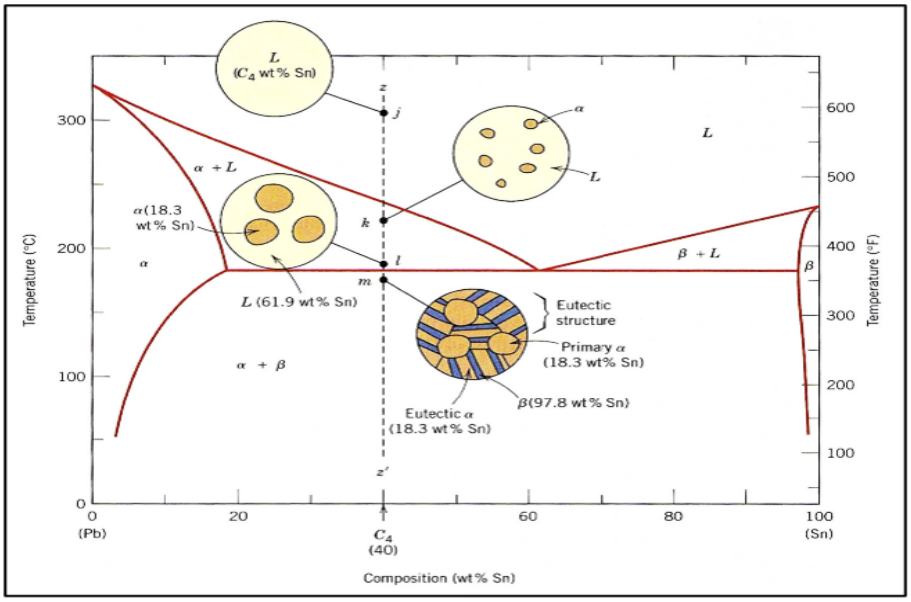

Figure 7: Phase diagram of Pb-Sn alloy and the microstructural Evolution at composition C4 (L denotes liquid).

In Figure.7, the microstructures at composition C4 have the following characteristics:

α+L zone

- When the temperature is lowered from liquid zone to α+L zone, there is a driving force to precipitate α crystals from liquid. In this case, α crystals are convex and close to spherical (to lower the molar total chemical potential due to the surface of α crystals).
- When the temperature is further lowered and the system is further away from liquid zone, the driving force to precipitate α crystals will increase. But the mobility of atomistic species is slower which is unfavorable to nucleation. Possibly due to this reason the density of α crystals at point I is apparently lower than that at point k.
- The composition of α crystals at point I is ~18.3 wt% Sn, whereas the composition of liquid is ~61.9 wt% Sn. According to lever rule: the ratio of α crystal at point l is higher than that of point k. All these results comply with the phase diagram shown in Fig.7.

α+β zone:

- In this case, the main driving force for phase transition is to form solid α and solid β crystals simultaneously from the rest liquid. The α crystals already appeared at point l remain at point m.
- The microstructure at point m shows: the α and β crystals transformed from liquid are with alternating lamellar structure. These new α crystals apparently have different shape from the α crystals already formed at point l. The shape of interweaving grains might be related to that solid α crystals and solid β crystals precipitate simultaneously where kinetics might be involved, e.g. diffusion.
- The α crystals in interweaving grains contain ~18.3 wt% Sn, while the β crystals contain ~97.8 wt% Sn, both complying with its phase diagram.
- When cooled from the Eutectic composition, since the solid α crystals and solid β crystals precipitate simultaneously with very different compositions, it's not surprising to see that α crystals and β crystals

appear with alternating lamellar structure (or rod-like), as reported in many studies.

Evolution of microstructure in a carbon steel

Fig.8 is a part of the phase diagram of a carbon steel and the microstructural evolutions at composition C0 [9].

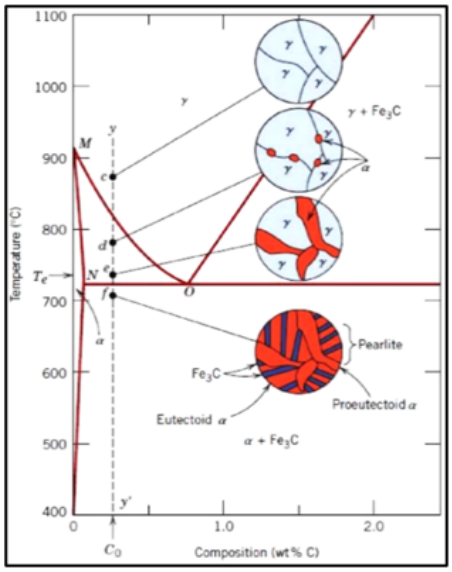

Figure 8: Part of Iron Carbon Phase Diagram and the Evolution of Microstructures at C0 (γ crystals is Austenite)

The characteristics of Fig.8 include:

The phase transition from point c to point d is to precipitate α crystals from the grain boundary of γ crystals where the molar total chemical potential is higher (because of less complete bonding). These α crystals are close to spherical to reduce the molar total chemical potential of α crystals.

The Proeutectoid α crystals at point e are not only larger, but also apparently deviate from being spherical. A logical reasoning is: the growth of Proeutectoid α crystals is along the boundaries of solid γ crystals where the molar total chemical potentials are higher, therefore are not near spherical any more. Similar to Fig.7, the density of Proeutectoid α crystals at point e is slightly lower than that at point d, while the ratio of Proeutectoid α crystal at point e is higher than that at point d, complying with lever rule.

As mentioned in 3.1(d), the Eutectoid α crystals simultaneously appearing with Fe_3C are with alternating lamellar structure.

Improvement of Properties via Microstructure

The microstructure of materials can be totally at equilibrium (a single crystal), nearly at equilibrium (poly-crystal), totally non-equilibrium or somewhere among them, and can have a morphology controlled by various mechanisms (e.g. cooling rate control, diffusion control and etc.). Therefore, the microstructural modification for better properties is a huge area. Some related researches are as follows:

Kathavate et al used additives in multilayered complex structures to improve their microstructures so that superior mechanical, thermal, chemical and physical properties can be obtained [10].

Wang et al investigate the relation among the microstructure of a titanium alloy, fracture toughness and crack propagation, and find a better combination of strength, ductility and fracture toughness [11].

The stability and lifetime of devices are related to the microstructures of materials, thus modifying microstructures is a means to improve the performance of devices. For example, Wong et al used diffusion-controlled morphology modification to improve the stability of organic photovoltaics [12].

Use of machine or AI in Designing Materials

In recent years, the use of machine or AI (artificial intelligence) as a tool to improve the microstructures and properties of materials is much valued. The following are related studies:

Whitman et al published a paper [13] stressed on the rise of computational materials science. The methods are based on the microstructure–property relationships from data. In addition, two case studies were demonstrated.

Madika et al published a review paper [14] on the recent impact of artificial intelligence (AI), machine learning (ML), and deep learning (DL) on materials science, emphasizing on materials discovery, development and optimization.

The author believes, if the users of these tools have better understanding of the Atomistic 2nd Law of Thermodynamics and of kinetics, their work would be more effective and better results could be obtained.

Discussion

T-T-T curve

In a typical T-T-T curve, the Y-axis is temperature and the X-axis is time. The 1st solid line shows "the time needed for the initiation of phase transition at various temperatures". The 2nd solid line shows "the time needed for 100% of phase transition at various temperatures". It is not hard to see that T-T-T curves are very different from phase diagrams in nature.

However, the driving force for both T-T-T curves and phase diagrams is "the lowering of molar total chemical potential of atomistic features", it's only natural that they have the same phase transitions. The following analyses of T-T-T curves are based on Atomistic 2nd Law of thermodynamics and kinetics.

T-T-T curve for 1080 steel

Fig.9 is the T-T-T curves for 1080 steel [15]. This T-T-T curves have the typical C-shape, and can be used as an example to elaborate on the characteristics of T-T-T curves:

The upper part of a T-T-T curve: Whether for 0%, 50% or 100%, the time needed for phase transitions are gradually prolonged as Eutectoid temperature (727°C) is approached, and phase transitions all stop at Eutectoid temperature. This phenomenon shows: the time needed for phase transition is inversely related to the driving force of atomic species. As a result, when the temperature is very close to Eutectoid temperature, the driving force of atomic species is ~0 and the time needed for phase transition is ~∞, even though the mobility of atomic species is higher at higher temperature.

(1) T-T-T curves: Whether for 0%, 50% or 100% phase transition, at the temperature somewhat lower than Eutectoid temperature, although the driving force for phase transitions is not the largest (smaller than lower temperatures), the time needed for phase transition is shorter than higher and lower temperatures. Hence, T-T-T curves have s at certain middle temperature, showing the combined effect of driving force and mobility is the largest at this middle temperature. Moreover, the of the first curve appears after a short time (not at 0 second). A logical explanation is: the phase transition of atomic species have to overcome the activation energy and need time to gather and nucleate.

The lower part of a T-T-T curve: Whether for 0%, 50% or 100%, although the decrease of temperature means further away from Eutectoid temperature and a higher driving force for phase transition. But the time needed

for phase transition is gradually prolonged. This phenomenon shows: in this condition the driving force of atomic species is not as important as their mobility; hence the time needed for phase transition is longer when the temperature and mobility are lower.

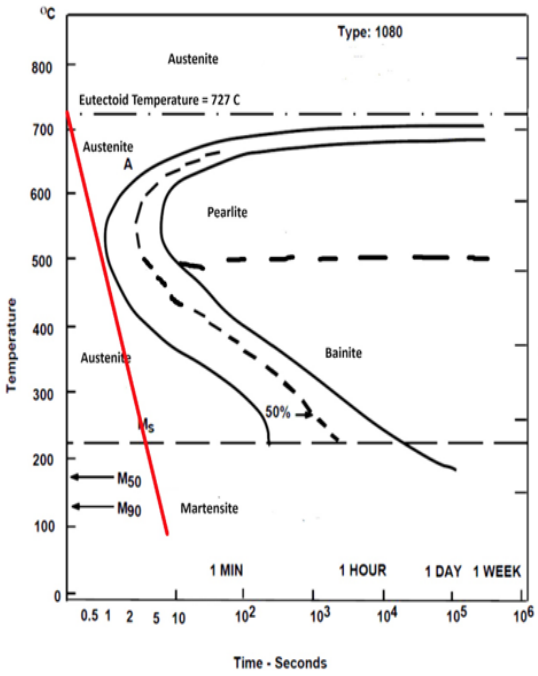

Figure 9: T-T-T curve for 1080 steel

The red line in Figure.9 does not touch the T-T-T curves of Pearlite or Bainite in 1080 steel, therefore only Martensite is formed during cooling. This Martensitic steel can be tempered to obtain the needed crystals of Pearlite or Bainite. Conversely, if the cooling of 1080 steel crosses the T-T-T curves of these crystals, the corresponding crystals will be formed.

T-T-T Curves for other Materials

T-T-T curves are often used for steels. Since the basic rules involved (i.e. the Atomistic 2nd of Thermodynamics and kinetics) are the same for other materials, similar T-T-T curves can be established and used. For example, Onike et al [16] established the T-T-T curves for Kaolinite in 1986, Liu [17] established the T-T-T curves for Kaolinite and Alumina in 1990; Long et al [18] used a T-T-T curve in the glass-forming ability of a metal alloy in 2009; Martín et al [19] used a T-T-T curve to depict the crystallization behavior of a glass fiber in 2014.

Contains Low-Melting Impurities

Ceramic raw materials normally contain low-melting impurities that will form liquid at low temperatures. When the cooling was fast enough, this liquid did not touch the T-T-T curves of its crystals, thus a co-existing glassy phase was formed. For example, there are small amounts of low-melting impurities in Kaolinite and Alumina materials, like K_2O (melting point~700°C), Na_2O (melting point~1132°C) or FeO (melting point<1400°C). When the mixture of Kaolinite and Alumina was reaction sintered at 1650°C to form mullite, a co-existing glassy phase would appear after cooling.

Fig.10 is a picture of DDF (Darkfield Diffraction) in TEM (Transmission Electron Microscopy) [17], showing the mullite crystals are surrounded by a glassy thin film and glassy pockets. This glassy phase comes from the low-melting impurities of raw materials.

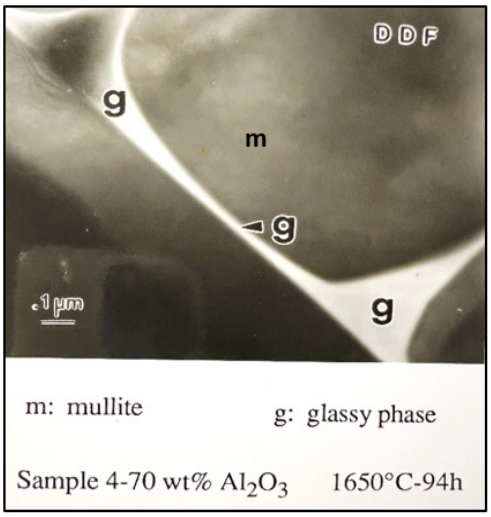

Figure 10: A TEM picture showing the mullite crystals (m) are surrounded by a glassy thin film and glassy pockets (g).

The mechanical property of impurity-containing glassy phase should not be important. Metallurgical slags contain many low-melting impurities left from metal making. Shang et al [19] systematically reviewed the advances in utilizing metallurgical slags to manufacture glass ceramics. Their emphases are on the challenges and solutions for maximizing utilization of these wastes with desirable product quality.

Du et al [21] used heavy metal containing blast furnace slag in the manufacture of high-performance glass ceramics. They observed that the leaching concentrations of Zn, Mn, Cr in products were much lower than the standard values of hazardous waste leaching toxicity. This indicated that these glass ceramics also have good curing effects.

Conclusion

The rule of the Atomistic 2nd Law of Thermodynamics for spontaneous equilibrium is: the molar total chemical potential in the system is the lowest. Its necessary and sufficient condition is: the co-existing phases at equilibrium have the same molar total chemical potential. These rules can be applied to the phase diagrams of single component (e.g. water or carbon) as well as to binary phase diagrams. The elaborated examples of these rules in binary phase diagrams are at Eutectic temperature, slightly higher than Eutectic temperature and slightly lower than Eutectic temperature. The common tangent and lever rule are also used in these binary examples.

In literature, the phase diagrams of Pb-Sn alloy and a carbon steel were displayed together with the microstructures at a composition. It is known from these phase diagrams that, the microstructures of precipitated crystals can be close to spherical or far away from spherical, can be with different sizes, with different densities, and with alternating lamellar structure. The author explains these phenomena rationally based on the Atomistic 2nd Law of Thermodynamics and kinetics.

The microstructure of a material can be totally at equilibrium (a single crystal), close to equilibrium (poly-crystal), or very far away from equilibrium, or somewhere among them, and can have a morphology controlled by various mechanisms. Therefore the range of microstructures is very wide. Since the microstructures of materials are closely related to their properties, in recent years the use of machine or AI for superior material properties is highly valued. The author believes, these tools should be more effective if the users are with a better understanding of the Atomistic 2nd Law of Thermodynamics and of kinetics.

T-T-T curves are to describe the time needed for certain degrees of phase transitions under various temperatures

in a system. Hence the dynamic nature of T-T-T curves is different from phase diagrams. From the viewpoints of driving force and mobility of atomistic species, the author explains the formation of a T-T-T curve in detail. The small amount of time needed to initiate these curves are explained via kinetics. Although T-T-T curves are often used in steel, the rules involved are also applicable to other materials.

The raw materials for ceramics normally contain low-melting impurities, hence liquid will appear at low temperatures. During cooling, this co-existing and enclosing liquid will form a glassy phase because it does not touch the T-T-T curves of its crystalline phase(s). Some metallurgical slags containing heavy metals can be used as the raw materials for high performance glass ceramics. The leaching concentrations of Zn, Mn, and Cr ions in products were much lower than the standards for hazardous waste leaching toxicity. Therefore, metallurgical slags can be reused for this value-added purpose without environmental concerns.

Conflicts of Interest

The author declares no conflicts of interest regarding the publication of this paper.

References

1. Kuo-Chung Liu (2025) Communication: A Simpler and More Applicable 2nd Law of Thermodynamics. Advances in Materials Physics and Chemistry 15: 3.
2. Kuo-Chung Liu (2025) Communication: Phenomena That Could Make the Atomistic 2nd Law of Thermodynamics Clearer, Advances in Materials Physics and Chemistry 15: 7.
3. Phase Diagram for Water https://courses.lumenlearning.com/umes-cheminter/chapter/phase-diagram-for-water/.
4. Wikipedia, Carbon, last edited on 6 March 2026, https://en.wikipedia.org/wiki/Carbon.
5. Phase-diagrams 2-Eeutectic reactions https://www.doitpoms.ac.uk/tlplib/phase-diagrams/phasediags2.php.
6. How to Read Ternary Phase Diagrams: A Guide, Published on 09 May 2025 https://scilift.blog/ternary-phase-diagrams.
7. Cuiping Wang, Xianjie Zhang, Lingling Li, Yunwei Pan et al, (2018) Phase Equilibria of the Co-Ti-Ta Ternary System, November, Metals 8: 11.
8. A Practical Guide to Phase Diagrams https://phasediagram.weebly.com/eutectics.html.
9. Diana Tsenenko, EXATIN INFORM, August 26, 2019, https://exatin.info/iron-carbon-phase-diagram/.
10. V S Kathavate and K Eswar Prasad (2025) Microstructure Evolution and Mechanical Properties of Alloys Fabricated via Additive.
11. Huan Wang, Qinyang Zhao, Shewei Xin, Yongqing Zhao, Wei Zhou,Weidong Zeng (2021) Microstructural morphology effects on fracture toughness and crack growth behaviors in a high strength titanium alloy, Materials Science and Engineering: A 821: 21.
12. Yiwen Wong, Huanhuan Gao, Min Sun, Chieh-Ting Lin, Hongxiang Li, Francis R. Lin, Baobing Fan, Zhe Li, Juan Antonio Zapien, Alex K.-Y. Jen (2025) Diffusion-Controlled Morphology Modification via Employing Host/Guest Acceptors to Improve the Stability of Organic Photovoltaics, Advanced Energy Materials 14: 19.
13. Sheila E Whitman and Marat I Latypov (2025) Machine learning of microstructure–property relationships in materials leveraging microstructure representation from foundational vision transformers, Acta Materialia 296.
14. Benediktus Madika, Aditi Saha, Chaeyul Kang, Batzorig Buyantogtokh, Joshua Agar, Chris M. Wolverton, Peter Voorhees, Peter Littlewood, Sergei Kalinin, Seungbum Hong (2025) Artificial Intelligence for Materials Discovery, Development, and Optimization, American Chemical Society.
15. Seth Price (2024) Reading a time temperature transformation curve for metallurgy https://insights.globalspec.com/article/22799/reading-a-time-temperature-transformation-curve-for-metallurgy.
16. F Onike, G D Martin, A C Dunham (1986) Time -Temperature-Transformation Curves for Kaolinite, Materials Science Forum 7.

17. Kuo-Chung Liu (1990) Ph.D. Thesis, Figure.3.7 of "Mullite Formation by Reaction Sintering of Kaolinite-Alumina", University of California at Berkeley.
18. Zhilin Long et al, (2009) On the new criterion to assess the glass-forming ability of metallic alloys, Materials Science and Engineering A 509: 23-30.
19. MI Martín, Felix A López, Francisco jose Alguacil, and Maximina Romero (2014) Development of crystalline phases in sintered glass-ceramics from residual E-glass fibres, Ceramics International 40: 2.
20. Wenxing Shang , Zhiwei Peng, Yawen Huang, Foquan Gu et al, (2014) Production of glass-ceramics from metallurgical slags, Journal of Cleaner Production 317: 1.
21. Yongsheng Du, Yuhang Guo, Guangyu Wang, Hongxia Zhang, Leibo Deng, et al. (2023) Preparation of glass–ceramics from blast furnace slag and its heavy metal curing properties 25: 3081-3092.